IEEE Access
Multidisciplinary | Rapid Review | Open Access Journal

Received August 22, 2020, accepted September 13, 2020, date of publication September 23, 2020, date of current version October 6, 2020.

Digital Object Identifier 10.1109/ACCESS.2020.3026143

New Local Region Based Model for the Segmentation of Medical Images

NOOR BADSHAH[1], HADIA ATTA[2], SYED INAYAT ALI SHAH[2], SOBIA ATTAULLAH[3], NASRU MINALLAH[4], (Member, IEEE), AND MATI ULLAH[1]

[1]Department of Basic Sciences, University of Engineering and Technology Peshawar, Peshawar 25120, Pakistan
[2]Department of Mathematics, Islamia College Peshawar, Peshawar 25120, Pakistan
[3]Department of Zoology, Islamia College Peshawar, Peshawar 25120, Pakistan
[4]Department of Computer Systems Engineering, University of Engineering and Technology Peshawar, Peshawar 25120, Pakistan

Corresponding author: Noor Badshah (noor2knoor@gmail.com)

ABSTRACT Segmentation of images having inhomogeneous intensities is always challenging. In this paper, we propose a model based on new local data statistics using local means and variances for detection of region of interest in medical images suffered from intensity inhomogeneity. This is done by introducing a new probability density function based on coefficient of variation, which is a best measure for inhomogeneous data. The new energy functional in the proposed model is then expressed in terms of level set function and is minimized for optimal energy. Minimization of the energy will lead to a partial differential equation, which is solved by using well known explicit method. Results of the proposed model are compared with other state of the art models and found that the proposed model outperform other existing models. Comparison is given in both qualitative and quantitative way. Furthermore, the proposed model is tested on different type of medical images like MRI, CT, Mammogram and skin lesion etc.

INDEX TERMS Gaussian processes, image segmentation, intensity inhomogeneity, level set method, variational techniques.

I. INTRODUCTION

Image segmentation is the process of semi-automatic or automatic detection of edges/region of interest based on intensity homogeneity, within an image for further analysis. Segmentation of images plays an important role in medical sciences. To deal with the medical images having tumors, an automatic detection of the tumor is one of the major and challenging task. A tumor, an abnormal growth of mass/tissues, needs to be detected critically and efficiently in order to increase the survival rate. The main difficulty with segmenting medical images having tumor is due to high variability in an image. Furthermore, different analysis itself indicates major modes of variation in intensities. Inhomogeneous intensity usually occurs in medical images such as Magnetic Resonance Imaging (MRI), Computed Tomography (CT), X-ray, Positron Emission Tomography (PET), Optical Coherence Tomography (OCT), Single Photon Emission Computed Tomography (SPECT), as a result of artifacts, the effects of illumination or technical limitations introduced by display objects. Inhomogeneous intensity is a smooth change in intensity within the original uniform region. The presence of inhomogeneous intensity in medical images can lead to misjudgment by doctors and researchers. The segmentation results can then be used to get additional diagnostic data. In this paper, our main focus is to develop a new active contour model for segmentation of medical images having intensity inhomogeneity.

Variety of mathematical models have been proposed for segmentation of images, which are mainly classified into two groups (i) Edge based active contour models (EBMs) (ii) and Region based active contour models (RBMs). The first group of models are using edge information (gradient) for detection of edges in the images [2]. These models are very sensitive to initialization and outliers (noise) in the image. While region based models use region statistics (like least square data fitting) for detection of region of interest in images [3].

One of the most known EBM is the geodesic active contour model [4], which has been efficiently applied for images with high dissimilarity in gradient at the object's edges. But the model may not produce satisfactory results in images having noise or blur [2]. Also this model is sensitive to initialization and may fall into local minima [17]. The above discussed shortcomings in the efficient use of EBM have limited their applicability in the field of image segmentation and lead

The associate editor coordinating the review of this manuscript and approving it for publication was Essam A. Rashed.

to the use of RBMs. Owing to the less sensitivity towards noise in the images [5] and no data required about image gradient, such models successfully allow the segmentation of objects with weak or no edges [15]. The significant features of RBMs can also automatically detect the interior contours and shows less dependency on the location of initial contour [15].

The first model of RBMs was introduced by Mumford and Shah (MS) [12], which illustrates that piecewise smooth intensity is appropriate for images having intensity inhomogeneity. However, MS model has some limitations due to which it is hard to minimize the energy functional. Since firstly, it is non-convex and may have several local minima. Secondly, the energy functional of MS model contains two unknowns both are of different nature. That is image (function of N dimensions) and curve ((N-1) dimensions) [16].

The Chan-Vese (CV) model is a special case of MS model, which divides given image into two parts i.e background and foreground [5]. CV model uses the global information of homogeneous regions outside and inside the evolving curve to identify objects whose boundaries may not be defined by gradient [6]. As a result, CV model has obtained outstanding segmentation result in images with weak or blur boundaries. Due to taking constant mean value in each region in a global framework, this model may not work efficiently in images with inhomogeneous intensity and images having clutter or complex background [6]. Li *et al.* [8] suggested local binary fitting (LBF) model for segmentation of images with inhomogeneous intensity.

LBF model utilizes two fitting functions that locally approximate the image intensities on the two sides of the contours. This model may produce better segmentation results of objects boundary completely due to local intensity information [1]. Though, it is delicate to the initial value on contours and is easy to capture into a local minimum [8], [10] and also not able to extract out the boundaries of objects with low contrast [11] which limit its realistic applications.

Wang *et al.* [1] proposed an active contour model driven by Local Gaussian Distribution Fitting (LGDF) energy with a level set function and local means and variances as variables. The local intensity means and variances are strictly derived from a variational principle, instead of being defined empirically. So it has shown certain ability of handling images having intensity inhomogeneity, noise and also identifying regions with different intensity variations. This model may not work very well in images having intensity inhomogeneity with complex/cluter background, which can be seen in experimental section IV. This model may not give good segmentation results in images of large sizes or may be very slow in convergence.

Badshah *et al.* [13] presented a selective segmentation model (CVES) based on coefficient of variation. The fitting term is based on coefficient of variation which is used to segment the image where regions are overlapping and have inhomogeneous intensities. CVES model works better for images with overlapping regions and intensity inhomogeneity [13]. But images having severe intensity inhomogeneity and is not able to segment the edges of the desired object.

Zhang *et al.* [14] proposed a region (local and global) based signed pressure force (SPF) model for image segmentation with a new level set method called selective binary and Gaussian filtering regularized level set (SBGFRLS) method. SBGFRLS model used the signed pressure force function as a region detector function. The main features of this model is that firstly the contour efficiently stop on fuzzy edges. Secondly, this model does not depend on initial contour and can detect the objects with exterior and interior boundaries. Thirdly, this model has both properties of selective local and global segmentation. Due to this property this model not only detect the required object but also detect the other objects as well.

Fang *et al.* [18] proposed a new model i.e. HRSPF model, which is driven by weighted hybrid region based SPF to segment images having inhomogeneous intensities and noise. In which they defined two weighted functions i.e. global region based SPF (GRSPF) and local region based SPF (LRSPF) functions which are based on normalized global intensity and normalized absolute local intensity differences respectively. By combining these functions and also introduced a force propagation function, this model is robust and is able to segment real images having inhomogeneous intensities and noise.

Liu *et al.* [19] proposed GLSPF model i.e. global and local signed energy based pressure force model. First a global signed energy based pressure force (GSPF) is introduced, which can enhance the robustness to initial contour. Secondly also introduced a local signed energy based pressure force (LSPF), which can handle images having inhomogeneous intensities and noise. The global and local image information is used for the global and local force propagation functions, respectively. Then automatically used the global and local variances to balance the weights of the GSPF and the LSPF, thus solve the problem of setting of parameters. Also applying a regularization term which is used to avoid the process of re-initialization and a penalty term which is used to smooth the level set function. This model is able to segment images having intensity inhomogeneity and noise.

Segmentation of images having inhomogeneous intensities is always challenging. In this paper, we propose a model based on new local data statistics using local means and variances for detection of region of interest in medical images suffered from intensity inhomogeneity. This is done by introducing a new probability density function based on coefficient of variation, which is a best measure for inhomogeneous data. The new energy functional in the proposed model is then expressed in terms of level set function and is minimized for optimal energy. Minimization of the energy will lead to a partial differential equation, which is solved by using well known explicit method.

In this paper, our main focus is to develop an active contour model for segmentation of medical images, which have intensity inhomogeneity with cluttered /complex background.

We have also improved the computational cost for segmentation of medical images having large sizes. The proposed model is based on new local data statistics by introducing new probability density function in terms of coefficient of variation. It is a well known fact that coefficient of variation fits data in a better way in images having intensity inhomogeneity as compare to variances. Furthermore, to extend the domain to the whole domain, the model is expressed in terms of the level set function. For optimal value of local intensity means, variances and level set function the energy functional of proposed model is minimized through Euler Lagrange equation. The results of the proposed model are compared quantitatively and qualitatively with other existing state of the art models i.e SBGFRLS, LGDF and CVES models. The proposed model has produced more desirable results in terms of Computational (CPU) time, Similarity coefficients and Evaluation metrics. The proposed model is tested on two types of medical data sets, where it produced better segmentation results. Firstly, the proposed model works very well with images having intensity inhomogeneity with complex background i.e. minimum, maximum or averaged intensity background. Secondly, the proposed model improves the computational cost and converges fast and also works well with images of large sizes.

The rest of this paper is designed in the following way: Discussion on existing models is given in Section II. In Section III the proposed model is described in details with implementation of an algorithm. Final experimental results and comparisons of medical images are given in Section IV along with quantitative results. Conclusion is presented in Section VI.

II. EXISTING LITERATURE

Here we give a brief discussion of existing state of the art models for segmentation of images, both for global and selective segmentation. Some of these models are taken as motivation for proposing a novel model and some are discussed for comparison with proposed model.

A. CHAN VESE (CV) MODEL

Chan and Vese (CV) [5] is a region based model which is using piecewise constant Mumford and Shah model [12] by restricted it to two regions. For given gray image $I_0 : \Omega \rightarrow R$, the following minimization problem is proposed $\underset{b_1,b_2,\Psi}{min} F_{CV}(b_1, b_2, \Psi)$ where

$$F_{CV}(b_1, b_2, \Psi) = \sum_{i=1}^{2} \lambda_i \int_\Omega |I_0 - b_i|^2 \chi_i(\Psi(x, y))dxdy + \nu \int_\Omega |\nabla \chi_1(\Psi(x, y))|dxdy, \quad i = 1, 2, \tag{1}$$

where Ψ is the level set and χ_1 and χ_2 are characteristic functions which are used as region descriptor. The optimal values of b_i can be obtained by

$$b_i(\Psi) = \frac{\int_\Omega I_0 \chi_i(\Psi)dxdy}{\int_\Omega \chi_i(\Psi)dxdy}, \qquad i = 1, 2.$$

The following Euler Lagrange equation is solved to get optimal Ψ as:

$$\frac{\partial \Psi}{\partial t} = -\sum_{i=1}^{2} \lambda_i \chi_1'(I_0 - b_i)^2 + \nu \chi_1' \nabla \cdot \left(\frac{\nabla \Psi}{|\nabla \Psi|}\right), \quad \text{in } \Omega \tag{2}$$

for $i = 1, 2$, with the homogeneous Neumann boundary condition and χ_1' is the derivative of characteristic functions. The CV model works well in images with noise. This model may not produce very good results in images having intensity inhomogeneity and is also computationally expensive [6].

B. LOCAL BINARY FITTING (LBF) ENERGY MODEL

CV model [5] uses constant average intensities in different regions so works well in images with homogeneity and may not produce good results in inhomogeneous images. For segmentation of images having inhomogeneous intensity, Li *et al.* proposed a model based on local binary fitting energy (LBF) [8]. The energy functional in terms of level set is given by:

$$\begin{aligned} F_{LBF}(g_1, g_2, \Psi) &= \sum_{i=1}^{2} \lambda_i \int_\Omega G_\sigma(x - y)|I_0 - g_i|^2 \chi_i(\Psi(x, y))dydx \\ &+ \nu \int_\Omega \chi_1(\Psi(x, y))|\nabla \Psi|dx \\ &+ \mu \int \frac{1}{2}(|\nabla \Psi| - 1)^2 dx, \quad x, y \; in \; \Omega, \end{aligned} \tag{3}$$

where G_σ is a Gaussian kernel with standard deviation σ which control the size of local region, g_i for $i = 1, 2$ are local intensity fitting functions. The optimal values of g_i can be obtained by:

$$g_i = \frac{G_\sigma * [I_0 \chi_i(\Psi)]}{G_\sigma * \chi_i(\Psi)}, \quad i = 1, 2.$$

The following partial differential equation is solved for optimal Ψ as:

$$\begin{aligned} \frac{\partial \Psi}{\partial t} &= -\sum_{i=1}^{2} \lambda_i \chi_1' \int_{\Omega_i} G_\sigma(y - x)|I_0 - g_i|^2 dy \\ &+ \nu \chi_1' \nabla \cdot \left(\frac{\nabla \Psi}{|\nabla \Psi|}\right) \\ &+ \mu\left(\nabla^2 \Psi - div\left(\frac{\nabla \Psi}{|\nabla \Psi|}\right)\right). \end{aligned} \tag{4}$$

The localization property of LBF energy allows it to give better segmentation results in images having inhomogeneous intensities. And because of localization: the model may easily stuck at local minima and is very sensitive to the initialization, which may lead towards wrong segmentation for different initialization of Ψ [7]. Also this model does not give good segmentation result in noisy images and having severe intensity inhomogeneity.

C. THE LOCAL GAUSSIAN DISTRIBUTION FITTING (LGDF) ENERGY MODEL

LBF model [8] uses information of the local intensity to segment images with inhomogeneous intensities, but may easily get stuck within local minima. So Wang *et al.* [11] proposed an active contour model driven by local Gaussian distribution fitting (LGDF) energy with local means and variances as variables. The energy functional in terms of level set formulation is given by:

$$F(u_1, u_2, \sigma_1^2, \sigma_2^2, \Psi) = \nu L(\Psi) + \mu P(\Psi) - \sum_{i=1}^{2} \int_\Omega G_\sigma(x-y) log f_i(I_0(y))\chi_i(\Psi)dy, \tag{5}$$

for $i = 1, 2$, where first term is the data fitting term, $G_\sigma(x-y)$ is a Gaussian kernel which is positive function with fixed parameter σ and logarithm function is used to convert the maximization problem into minimization. Second and third terms are the length and re-initialization terms which can be defined as $L(\Psi) = \int |\nabla\chi(\Psi(x))|dx$ and $P(\Psi) = \frac{1}{2}\int(|\nabla\Psi(x)| - 1)^2\, dx$ respectively. Also f_i for $i = 1, 2$ are the probability density functions and are given by:

$$f_i(I_0(y)) = \frac{1}{\sqrt{2\pi}\sigma_i(x)} exp\left(\frac{-(u_i(x) - I_0(y))^2}{2\sigma_i(x)^2}\right), \quad i = 1, 2.$$

Minimizing the energy functional (5) w.r.t σ_i and u_i for $i = 1, 2$, we get:

$$\sigma_i(x)^2 = \frac{\int G_\sigma(y-x) * [(u_i(x) - I_0(y))^2\chi_i(\Psi)]dy}{\int G_\sigma(y-x) * [\chi_i(\Psi)]dy},$$

and

$$u_i(x) = \frac{\int G_\sigma(y-x) * [I_0(y)\chi_i(\Psi)]dy}{\int G_\sigma(y-x) * [\chi_i(\Psi)]dy}.$$

By keeping fixed $\sigma_i(x)^2$ and $u_i(x)$, we minimize (5) w.r.t Ψ and can be obtained

$$\begin{aligned}\frac{\partial\Psi}{\partial t} &= -\sum_{i=1}^{2}\chi_1'\int_\Omega G_\sigma(y-x)\left[log(\sigma_i(y)) + \frac{(u_i(y) - I_0(x))^2}{2\sigma_i(y)^2}\right]dy \\ &\quad + \nu\chi_1'\nabla\cdot\left(\frac{\nabla\Psi}{|\nabla\Psi|}\right) \\ &\quad + \mu\left(\nabla^2\Psi - div\left(\frac{\nabla\Psi}{|\nabla\Psi|}\right)\right), \quad for\ i = 1, 2. \end{aligned} \tag{6}$$

LGDF model works efficiently in the segmentation of images with different regions having inhomogeneous intensities. Firstly, this model may not work very effectively with images having severe inhomogeneous intensities, complex background (i.e. with maximum or minimum intensity background) and severe noise. Secondly, LGDF model may stuck within local minima [9]. Thirdly the computational cost of LGDF model increases with an increase in the size of images.

D. THE COEFFICIENT OF VARIATION EQUIPPED SELECTIVE (CVES) MODEL

Badshah *et al.* [13] proposed a selective segmentation model based on geometrical constraints, while the fitting term is based on coefficient of variation to segment images having overlapping regions and images with inhomogeneous intensity. The following minimization problem $\min_{b_1,b_2,\Psi} F_{CVES}(b_1, b_2, \Psi)$ is as follows:

$$\begin{aligned}F_{CVES}(b_1, b_2, \Psi) &= \sum_{i=1}^{2}\lambda_i\int_\Omega\frac{(I_0 - b_i)^2}{b_i^2}\chi_i(\Psi)dxdy \\ &\quad + \mu\int_\Omega d(x,y)g(|\nabla I_0|)\chi_1(\Psi)|\nabla\Psi|dxdy,\end{aligned} \tag{7}$$

where $i = 1, 2$ and b_i can be found by:

$$b_i(\Psi) = \frac{\int_\Omega I_0^2(x,y)\chi_i(\Psi)dxdy}{\int_\Omega I_0(x,y)\chi_i(\Psi)dxdy}, \qquad i = 1, 2.$$

By keeping b_i fixed, the minimization of energy functional (7) w.r.t Ψ is given as:

$$\begin{aligned}\frac{\partial\Psi}{\partial t} &= \nu\chi_1'\nabla\cdot\left(d(x,y)g(|\nabla I_0|)\frac{\nabla\Psi}{|\nabla\Psi|}\right) \\ &\quad - \sum_{i=1}^{2}\lambda_i\chi_1'\frac{(I_0 - b_i)^2}{b_i^2}.\end{aligned} \tag{8}$$

By adding balloon term $\alpha d(x,y)g(|\nabla I_0|)|\nabla\Psi|$ in above (8) is used to speed up the convergence of the evolution.

$$\begin{aligned}\frac{\partial\Psi}{\partial t} &= \nu\chi_1'\nabla\cdot\left(d(x,y)g(|\nabla I_0|)\frac{\nabla\Psi}{|\nabla\Psi|}\right) \\ &\quad - \sum_{i=1}^{2}\lambda_i\chi_1'\frac{(I_0 - b_i)^2}{b_i^2} \\ &\quad + \alpha d(x,y)g(|\nabla I_0|)|\nabla\Psi|, \quad in \quad \Omega, \\ \Psi(t,x,y) &= \Psi_0(x,y), \quad in\ \Omega.\end{aligned} \tag{9}$$

CVES model has a better performance in images having overlapping regions and images having inhomogeneous intensity [13]. This model may produce leakages through edges in images with severe inhomogeneous intensity.

E. ACTIVE CONTOURS WITH SELECTIVE LOCAL OR GLOBAL SEGMENTATION: A NEW FORMULATION AND LEVEL SET (SBGFRLS) METHOD

Zhang *et al.* [14] proposed a region (local and global) based model for image segmentation with a new level set method called selective binary and Gaussian filtering regularized level set (SBGFRLS) method. Firstly selective step was used to penalize the level set function to binary and then for the regularization Gaussian filter was used. The main purpose of Gaussian filter is that the evolution become more stable and also makes level set function smooth. Furthermore SBGFRLS model combines both the properties of Geodesic active contour (local segmentation) and Chan-Vese (global segmentation) models. The final evolution equation for the SBGFRLS model is defined as:

$$\frac{\partial \Psi}{\partial t} = \alpha |\nabla \Psi| \cdot spf(I_0(x)), \quad x \in \Omega, \tag{10}$$

where

$$spf(I_0(x)) = \frac{I_0 - \frac{(b_1+b_2)}{2}}{max\left(I_0 - \frac{(b_1+b_2)}{2}\right)}$$

and α controls the propagation of the contour. This SBGFRLS model is more efficient and accurate than geodesic active contour and CV models [14]. This model may not yield very good results in images having inhomogeneous intensity and complex background.

F. ACTIVE CONTOUR DRIVEN BY WEIGHTED HYBRID SIGNED PRESSURE FORCE (HRSPF) MODEL FOR IMAGE SEGMENTATION

Fang et al. [18] proposed a new weighted hybrid region (local and global) based SPF model i.e. HRSPF model for image segmentation. HRSPF model uses both GRSPF and LRSPF functions based on global and local information. First the GRSPF is used which is based on global pixel information which avoids the difficulty in the setting of parameters and enhance the capability of handling the images having inhomogeneous intensities. Similarly LRSPF is used by introducing the normalized absolute local intensity differences of the outer and inner local regions of the evolving curve. Also introduced a force propagation function which is based on the information of global image which can be used to automatically change the force during iteration. The final evolution equation for the HRSPF model is defined as:

$$\begin{aligned}\frac{\partial \Psi}{\partial t} &= |b_1 + m - 2b_2| \cdot |\nabla \Psi| \\ &\cdot\left(w_l \cdot \min\left(1, \frac{\max(|spf_{LR}(I_0(x))|)}{\max spf}\right)\right. \\ &\cdot spf_{LR}(I_0(x)) + w_g \cdot \min\left(1, \frac{\max(|spf_{GR}(I_0(x))|)}{\max spf}\right) \\ &\left.\cdot spf_{GR}(I_0(x))\right),\end{aligned} \tag{11}$$

where b_1 and b_2 are the average intensities as defined in [5], w_l and w_g are two weighted variables used to balance the effects of the functions of LRSPF and GRSPF, spf_{GR} and spf_{LR} represents the GRSPF and LRSPF functions respectively and $\max spf = \max(|spf_{GR}(I_0(x)), spf_{LR}(I_0(x))|)$ is the maximum absolute value of the GRSPF and the LRSPF functions.

This HRSPF model has the capability to control the pressure sign and implicitly control the evolution of the curve. And also contour expands and shrinks if it is inside and outside the object of interest respectively [18]. This model is not able to segment the region of interest having severe inhomogeneous intensities and severe noise.

G. A NOVEL ACTIVE CONTOUR MODEL GUIDED BY GLOBAL AND LOCAL SIGNED ENERGY BASED PRESSURE FORCE (GLSPF) MODEL

Liu et al. [19] proposed a novel GLSEPF model based on both global and local signed energy based pressure force model. Both global and local signed energy based pressure forces (GSPF and LSPF) are introduced, which can enhance the robustness to initial contour and can handle images having inhomogeneous intensities and noise. To avoid the problem of parameters setting, automatically used the global and local variances, which are used to balance the weights of the GSPF and the LSPF. Then combine both regularization and penalty terms. The final evolution equation for the GLSEPF model is defined as:

$$\begin{aligned}\frac{\partial \Psi}{\partial t} &= w_l \cdot \left[E_2^l(I_0(x)) - E_1^l(I_0(x))\right] \\ &\cdot \nabla \Psi + w_g \cdot \frac{\nabla E^g(I_0(x))}{\max\left(|\nabla E^g(I_0(x))|\right)} \\ &\cdot |b_1 - b_2| \cdot \nabla \Psi + \nu \chi_1' \nabla \cdot \left(\frac{\nabla \Psi}{|\nabla \Psi|}\right) \\ &+ \mu\left(\nabla^2 \Psi - div\left(\frac{\nabla \Psi}{|\nabla \Psi|}\right)\right),\end{aligned} \tag{12}$$

where w_l and w_g are two weighted variables, b_1 and b_2 are the average intensities, $\nabla E^g(I_0(x))$ is the difference of the global energy and $E_1^l(x)$, $E_2^l(x)$ are two local energy function.

This model is able to segment images having intensity inhomogeneity as well as noise [19]. But images having severe intensity inhomogeneity and severe noise, this model is not able to segment the region of interest.

III. THE PROPOSED MODEL

The LGDF model [11] can use the fitting energy of the local Gaussian distribution to separate regions with same average intensity but different variances. But LGDF model [11] is not able to acquire precise results when the images have severe intensity inhomogeneity and severe noise. In medical images it is hard to get precise segmentation results of images with severe intensity inhomogeneity and time consuming because these images with inhomogeneous intensities are always complex and large in size. In order to reduce the impact of severe inhomogeneous intensity, we propose a novel active contour model in which the local image intensities are based on means and variances which can rapidly segment the images having severe inhomogeneous intensities and also obtain accurate results. The coefficient of variation is the ratio of standard deviation to the mean and is widely used to get unit free measure of dispersion in the data. It can be very useful for comparing the variability between groups of observations. The coefficient of variation can be used both as a fidelity term and as a good region detector. We introduce a new local statistic (squared coefficient of variation) in local framework i.e. a new local intensity data fitting with the following probability density function:

$$f_{\{i,x\}}(I_0(y)) = \frac{1}{\sqrt{2\pi}\sigma_i(x)u_i(x)} exp\left(\frac{-(u_i(x)-I_0(y))^2}{2\sigma_i(x)^2u_i(x)^2}\right), \tag{13}$$

where σ_i and u_i for $i = 1, 2$ are spatially varying local variances and means respectively. To convert the model from maximization to minimization we take the logarithm of the probability density function, so we have the following energy functional for minimization as:

$$E = \sum_{i=1}^{2}\int_{\Omega_i} -G_\sigma(x-y)logf_{\{i,x\}}(I_0(y))dy, \tag{14}$$

where $G_\sigma(x-y)$ is a kernel, which takes a non-zero value in the neighborhood of x and zero otherwise. Thus we propose the following minimization problem in terms of the level set function and using length term and re-initialization of level set:

$$\begin{aligned}
&E(u_1, u_2, \sigma_1^2, \sigma_2^2, \Psi)\\
&= \int_\Omega\Big[-\int_{\Omega 1} G_\sigma(x-y)log\Big[\frac{1}{\sqrt{2\pi}\sigma_1(x)u_1(x)}\\
&\quad\times exp\left(\frac{-(u_1(x)-I_0(y))^2}{2\sigma_1(x)^2\,u_1(x)^2}\right)\Big]\chi_1(\Psi(y))dy\\
&\quad-\int_{\Omega 2} G_\sigma(x-y)log\Big[\frac{1}{\sqrt{2\pi}\sigma_2(x)u_2(x)}\\
&\quad\times exp\left(\frac{-(u_2(x)-I_0(y))^2}{2\sigma_2(x)^2\,u_2(x)^2}\right)\Big]\chi_2(\Psi(y))dy\Big]dx\\
&\quad+\nu\int|\nabla\chi_1(\Psi(x))|dx+\mu\int\frac{1}{2}(|\nabla\Psi(x)|-1)^2\,dx.
\end{aligned}$$

Or

$$\begin{aligned}
&\min_{u_1,u_2,\sigma_1^2,\sigma_2^2,\Psi} E(u_1, u_2, \sigma_1^2, \sigma_2^2, \Psi)\\
&= \int_\Omega\int G_\sigma(x-y)\Big(log\sqrt{2\pi}+log(\sigma_1)\\
&\quad+log(u_1)+\frac{(u_1-I_0(y))^2}{2\sigma_1^2u_1^2}\Big)\chi_1(\Psi(y))dxdy\\
&\quad+\int_\Omega\int G_\sigma(x-y)\Big(log\sqrt{2\pi}+log(\sigma_2)\\
&\quad+log(u_2)+\frac{(u_2-I_0(y))^2}{2\sigma_2^2u_2^2}\Big)\chi_2(\Psi(y))dxdy\\
&\quad+\nu\int|\nabla\chi_1(\Psi(x))|dx+\frac{\mu}{2}\int(|\nabla\Psi(x)|-1)^2dx,
\end{aligned}\tag{15}$$

where u_i and σ_i for $i = 1, 2$ may be computed by using following:

$$u_i = \frac{\int G_\sigma(y-x)*[I_0(y)^2\chi_i(\Psi(y))]dy}{\int G_\sigma(y-x)*[I_0(y)\chi_i(\Psi(y))]dy}, \tag{16}$$

and

$$\sigma_i^2 = \frac{\int G_\sigma(y-x)*[(u_i-I_0(y))^2\chi_i(\Psi(y))]dy}{\int G_\sigma(y-x)*[u_i^2\chi_i(\Psi(y))]dy}. \tag{17}$$

Now keeping u_i and σ_i fixed and minimizing the final energy functional $E(u_1, u_2, \sigma_1^2, \sigma_2^2, \Psi)$ w.r.t Ψ, we get the following Euler-Lagrange equation for Ψ:

$$\begin{aligned}
&-\chi_1'\int_\Omega G_\sigma(y-x)\Big[log(\sigma_1(y))+log(u_1(y))\\
&\qquad+\frac{(u_1(y)-I_0(x))^2}{2\sigma_1^2(y)u_1^2(y)}\Big]dy\\
&\qquad+\chi_1'\int_\Omega G_\sigma(y-x)\Big[log(\sigma_2(y))+log(u_2(y))\\
&+\frac{(u_2(y)-I_0(x))^2}{2\sigma_2^2(y)u_2^2(y)}\Big]dy\\
&+\nu\chi_1'\nabla\cdot\left(\frac{\nabla\Psi}{|\nabla\Psi|}\right)+\mu\left(\nabla^2\Psi-div\left(\frac{\nabla\Psi}{|\nabla\Psi|}\right)\right)=0, \quad in\ \Omega\\
&\frac{\chi_1'}{|\nabla\Psi|}\frac{\partial\Psi}{\partial\vec{n}}=0,\ on\ \partial\Omega\\
&\Psi(0,x,y)=\Psi_0(x,y), \quad in \quad \Omega.
\end{aligned}\tag{18}$$

with initial and boundary conditions. Eq. (18) may be considered as the steady state solution of the following partial differential equation

$$\begin{aligned}
\frac{\partial\Psi}{\partial t} &= -\chi_1'\int_\Omega G_\sigma(y-x)\Big[log(\sigma_1(y))+log(u_1)\\
&\qquad+\frac{(u_1(y)-I_0(x))^2}{2\sigma_1^2(y)u_1^2(x)}\Big]dy\\
&\quad+\chi_1'\int_\Omega G_\sigma(y-x)\Big[log(\sigma_2(y))\\
&\qquad+log(u_2)+\frac{(u_2(y)-I_0(x))^2}{2\sigma_2^2(y)u_2^2(x)}\Big]dy\\
&\quad+\nu\chi_1'\nabla\cdot\left(\frac{\nabla\Psi}{|\nabla\Psi|}\right)+\mu\left(\nabla^2\Psi-div\left(\frac{\nabla\Psi}{|\nabla\Psi|}\right)\right),
\end{aligned}\tag{19}$$

with homogeneous Neumann boundary conditions. The partial differential equation (19) is solved by simple and conditionally stable explicit method. The main steps of the proposed method are given in the following algorithm:

A. ALGORITHM

Algorithm 1 An Algorithm for the Evolution of Level Set Through Proposed Model

1) Input: Parameters α, μ, ν etc.
2) For given initial Ψ, find σ_i, u_i by using (16) and (17).
3) Use updated values of Ψ, find σ_i, u_i and solve (19) to update Ψ.
4) If required results are obtained stop the iterations otherwise go to step 1.
5) Output: Segmented result.

Various steps of the proposed model are illustrated in block diagram as shown in Fig. 1.

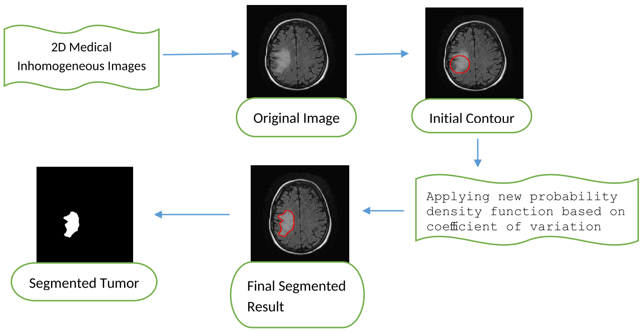

FIGURE 1. Block diagram of the proposed model.

In the next section we give experimental results of the proposed model on different type of medical images and compared the qualitative and quantitative results of the proposed model with a different state of the art models.

IV. EXPERIMENTAL RESULTS

In this section, experimental results of the proposed model on different types of medical images like mammogram images, MRI, Cardiac Magnetic Resonance (CMR) images is mention. All experimental tests are carried out by using Matlab 2010b. The proposed model on medical images taken from the website and two different datasets i.e. Montreal Neurological Institute's Brain Images of Tumors for Evaluation (MNI BITE) [20] and Radau *et al.* [21]. All these images have different level of intensity inhomogeneity with complex backgrounds. The experimental results of the proposed model are compared with three different existing state of the art models SBGFRLS, LGDF, CVES, HRSPF and GLSPF qualitatively and quantitatively.

The proposed model is using the following parameters σ, α and ν, which effects the final segmentation results by changing their values. In all experiments we used the parameters $\Delta t = 0.1$, $\lambda_1 = \lambda_2 = 1$, $\mu = 1$, $\nu = 0.001 \times 256 \times 256$ and the rest of parameters are adjusted according to the image. The Gaussian kernel G_σ is a scale parameter with standard deviation σ and α is also a scaling constant which are used to control the region scalability from small neighborhoods to the whole domain of the image and size of local region respectively. A small value of σ may cause undesirable results, detect unwanted regions and convergence is slow, whereas for large value of σ may cause high computational complexity. So the value of σ should be appropriately selected according to the image.

A. QUALITATIVE RESULTS

In this section we compared our proposed model qualitatively with other existing state of the art models. In all experiments from Fig. 2 to 8, Fig. (a) shows the original image with initial contour, (b), (c), (d), (e), (f) and (g) shows segmented results of SBGFRLS, LGDF, CVES, HRSPF, GLSPF and proposed models, respectively. We have used optimal (best) values of the parameters involved in each model.

Fig. 2 shows the mammogram image in which region of interest is a tumor with complex background. In Fig. 2b, the tumor is not detected correctly after 2000 iterations, in Fig. 2c the tumor is detected successfully, but some extra/unwanted region is also detected after 50 iterations. In Fig. 2d the segmented result is not satisfactory and have multiple local minima after 1000 iterations. Fig. 2e and 2f shows the results of WRSPF and GRSPF models respectively, which lead to unsuccessful results, because these models are unable to segment the region of interest in the given image. In Fig. 2g, experimental result of the proposed model is given, where the tumor is detected efficiently in only 15 iterations. Result showed the better performance of the proposed model in Fig. 2 over the existing models as SBGFRLS, LGDF, CVES, HRSPF and GLSPF models take a large number of iterations to converge.

Figure 3 demonstrates the segmentation results of real brain MRI image taken from free available data set the Montreal Neurological Institute's Brain Images of Tumors for Evaluation (MNI BITE) database [20]. In Fig. 3b and Fig. 3c the tumor is not segmented accurately and also some unwanted regions is segmented as well by SBGFRLS model and LGDF models respectively. In Fig. 3d, it can be seen that CVES model is able to detect the edges of tumor but it takes large number of iterations and CPU time. Fig. 3e and 3f shows the segmentation results of HRSPF and GLSPF respectively, where these models are not able to complete the task, give inaccurate results and also detect other undesired regions. Whereas our proposed model efficiently and accurately extracts the edges of tumor and it takes less number of iterations to converge (Fig. 3g) as compared to other existing models.

Figure 4 and Fig. 5 shows the experimental results of the segmentation of brain tumor having intensity inhomogeneity by SBGFRLS, LGDF, CVES and the proposed model. The original image with initial contour in Fig. 4a and Fig. 5a are brain MRI images of two different patients taken from the local hospital of Pakistan. In both images the intensities in background is inhomogeneous and the intensities of tumors are very close to background. The final segmentation results of SBGFRLS model are shown in Fig. 4b and Fig. 5b, where it can be shown that in both MRI images the results were unsatisfactory after 600 and 2000 number of iterations respectively. Figure 4c and Fig. 5c shows the final segmentation result of LGDF model after 960 and 900 iterations respectively. Both images show that the segmented results are not satisfactory because tumors as well as some extra region other than tumors are also detected. Figure 4d and Fig. 5d shows the final segmentation result of CVES model which is obtained after 1000 and 500 iterations respectively, the results are not satisfactory and also detect unwanted regions. Fig. 4e, 5e and 4f, 5f shows the segmentation results of HRSPF and GLSPF models respectively, where both models fail to detect the region of interest and detect the unwanted regions/boundaries. The final segmentation results of the proposed model are shown in Fig. 4g and Fig. 5g,

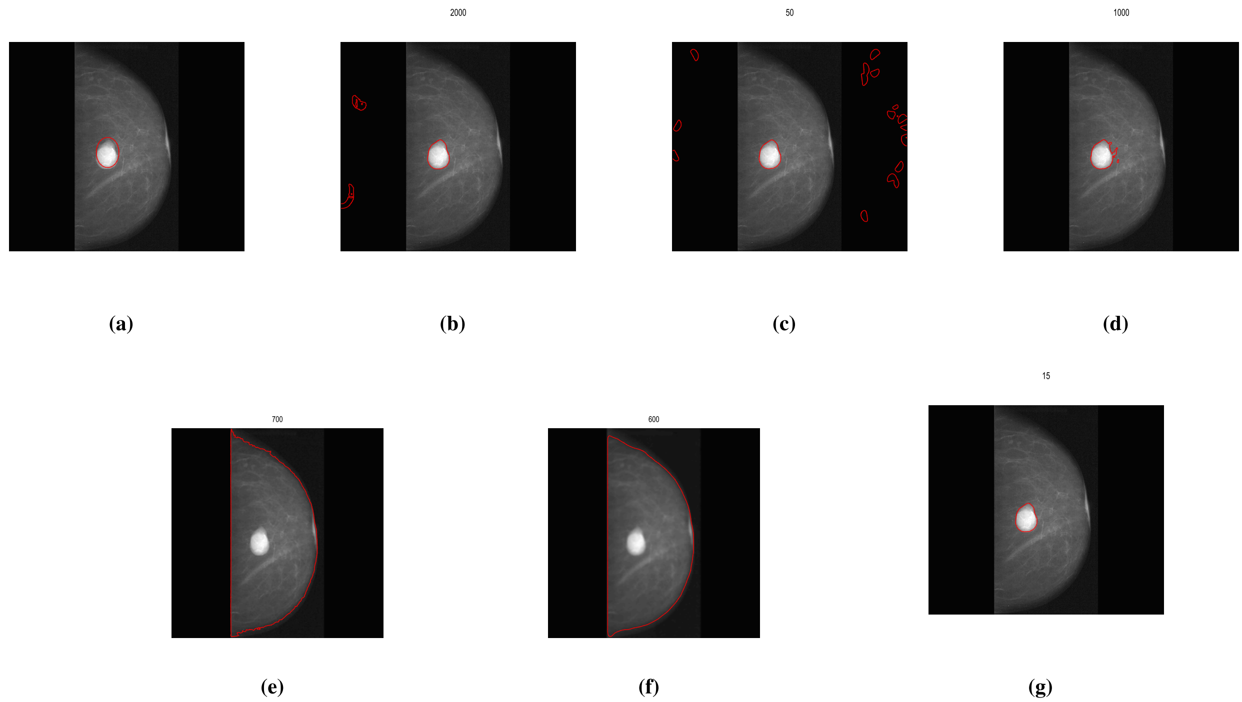

FIGURE 2. Detection of tumor in a mammogram image which has intensity inhomogeneity and complex background (a) original image with initial contour and (b)-(g) shows the segmented results by SBGFRLS, LGDF, CVES, HRSPF, GLSPF and proposed models.

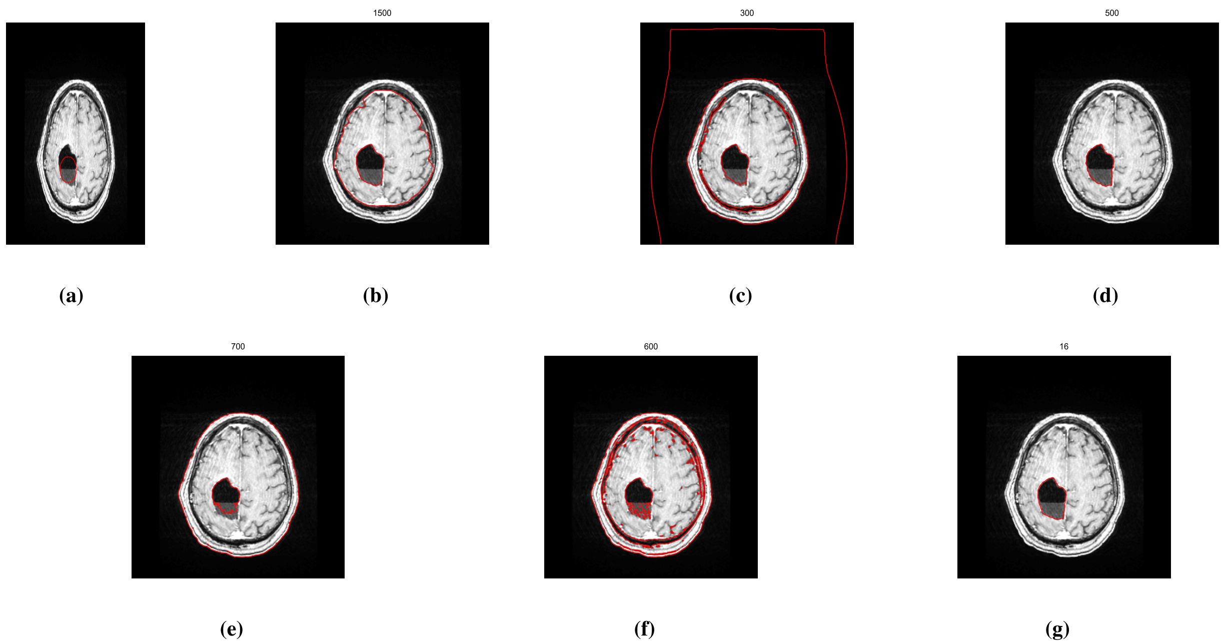

FIGURE 3. Segmentation of region of interest (tumor) in MRI image taken from dataset [20] (a) original image with initial contour and (b)-(g) shows the segmented results by SBGFRLS, LGDF, CVES, HRSPF, GLSPF and proposed models.

where both tumors of interest has been segmented accurately after 30 and 22 iterations respectively. From these results, it can be seen that the proposed model works very well with brain MRI images having intensity homogeneity and also detect the region of interest in less number of iterations and CPU time.

Figure 6 is a Cardiac magnetic resonance (CMR) image where the region of interest is left ventricle of heart which has intensity inhomogeneity, noise and complex background. The existing models have segmented the region of interest but some extra unnecessary regions are also detected while the proposed model has segmented the region of interest

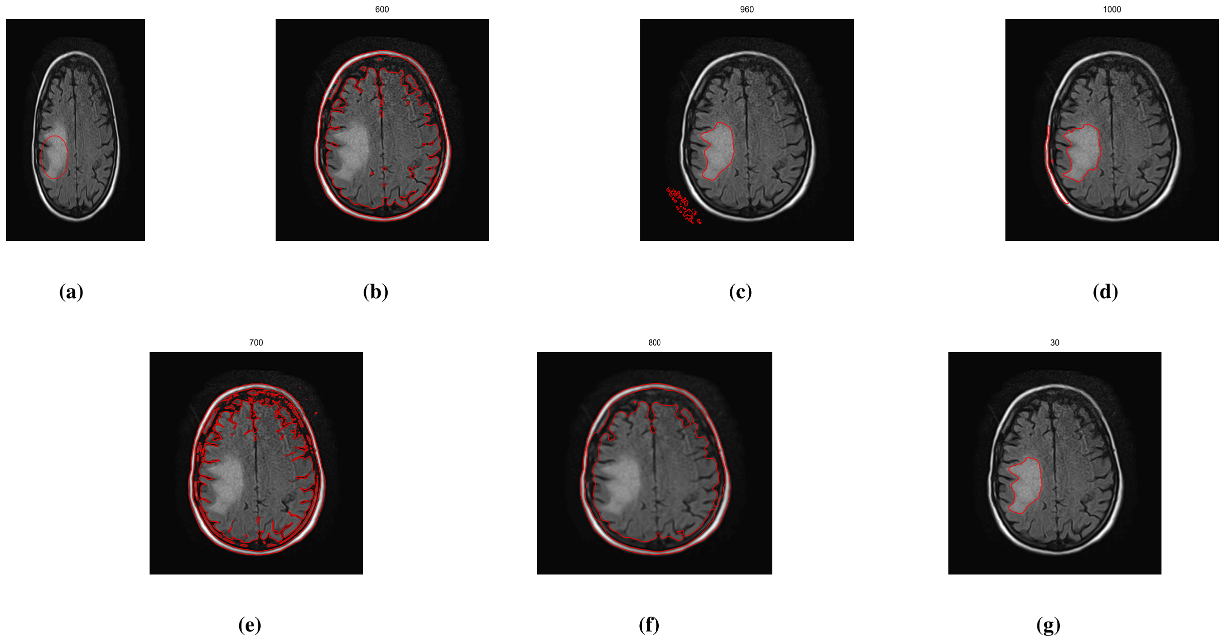

FIGURE 4. Comparison of proposed model with other existing models on brain MRI image taken from local hospital in Pakistan (a) original image with initial contour and (b)-(g) shows the segmented results by SBGFRLS, LGDF, CVES, HRSPF, GLSPF and proposed models.

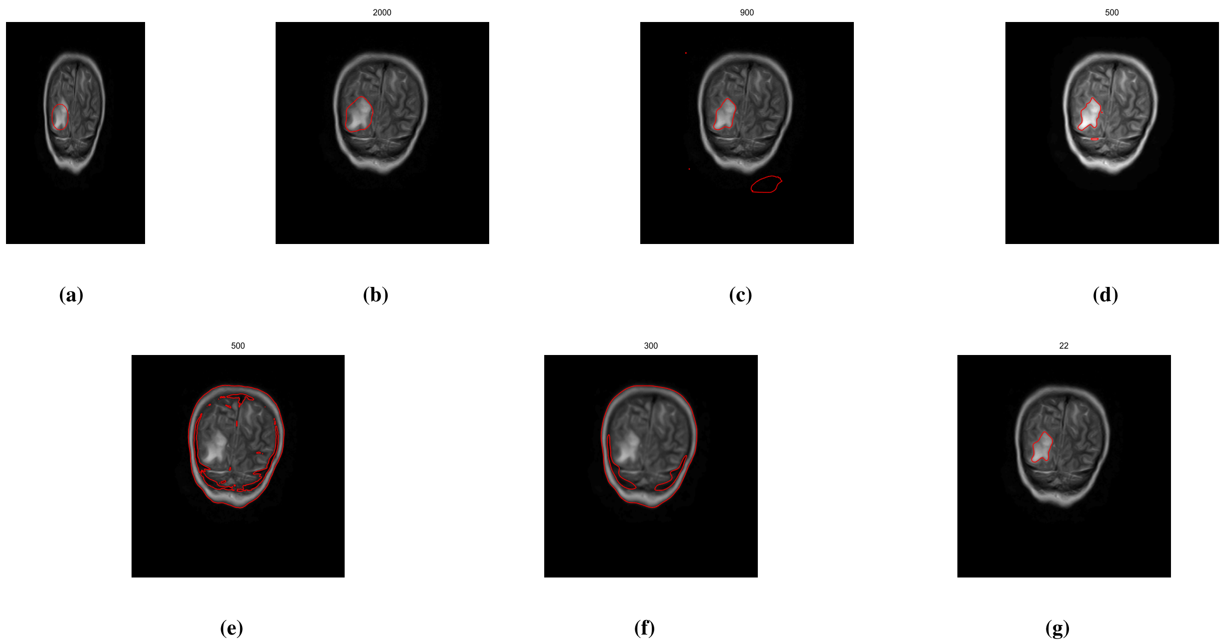

FIGURE 5. Comparison of proposed model with other existing models on brain MRI image taken from local hospital in Pakistan (a) original image with initial contour and (b)-(g) shows the segmented results by SBGFRLS, LGDF, CVES, HRSPF, GLSPF and proposed models.

accurately. The proposed model has given the required results in less number of iterations.

Figure 7 is a CMR image taken from the free available data set of Radau *et al.* [21] having intensity inhomogeneity and has minimum intensity in background. The better performance of the proposed model over other models can be seen in Fig. 7g.

In Fig. 8, experimental results of all the six models are given on a MRI images where the region of interest is the tumor. All models have performed better segmentation results, but the proposed model has produced the required results in less number of iterations and computational (CPU) time in seconds as shown in Fig. 8g. The efficiency of the images is extremely affected by the parameters σ and α.

TABLE 1. Comparison of SBGFRLS, LGDF, CVES, HRSPF and GLSPF models with the proposed model quantitatively in terms of number of iterations and CPU time (in seconds).

Medical Images	SBGFRLS model		LGDF model			CVES model		HRSPF model		GLSPF model		Proposed model		
	It	CPU	σ	It	CPU	It	CPU	It	CPU	It	CPU	σ	It	CPU
Fig. 1	2000	270	8	50	65	1000	1163	700	697	600	257	15	15	19
Fig. 2	1500	248	26	300	91	500	150	700	152	300	1993	26	16	3.6
Fig. 3	600	47	10	960	178	1000	315	700	1010	800	3229	13	30	9
Fig. 4	2000	241	10	900	257	500	170	500	2558	300	115	5	22	6
Fig. 5	1000	52	30	500	20	900	120	150	48	500	4209	17	40	5
Fig. 6	1000	47	10	500	42	250	80	500	242	600	654	10	70	14
Fig. 7	1500	155	5	250	8	1500	460	200	118	300	162	15	20	3

TABLE 2. Comparison of proposed model with other models on different image sizes of Figure 5.

Fig. 4	LGDF model		SBGFRLS model		CVES model		HRSPF model		GLSPF model		Proposed model	
Image Sizes	It	CPU	It	CPU	It	CPU	It	CPU	It	CPU	It	CPU
119 x 109	250	6.6	345	20	300	40	200	90	350	75	25	2.5
256 x 256	300	26	454	34	380	63	600	230	500	150	100	15
512 x 512	1000	642	1213	640	1478	1667	1150	947	1700	1265	850	490
1024 x 1024	1500	5459	2341	3210	3346	3456	4050	6543	5500	4350	1000	600

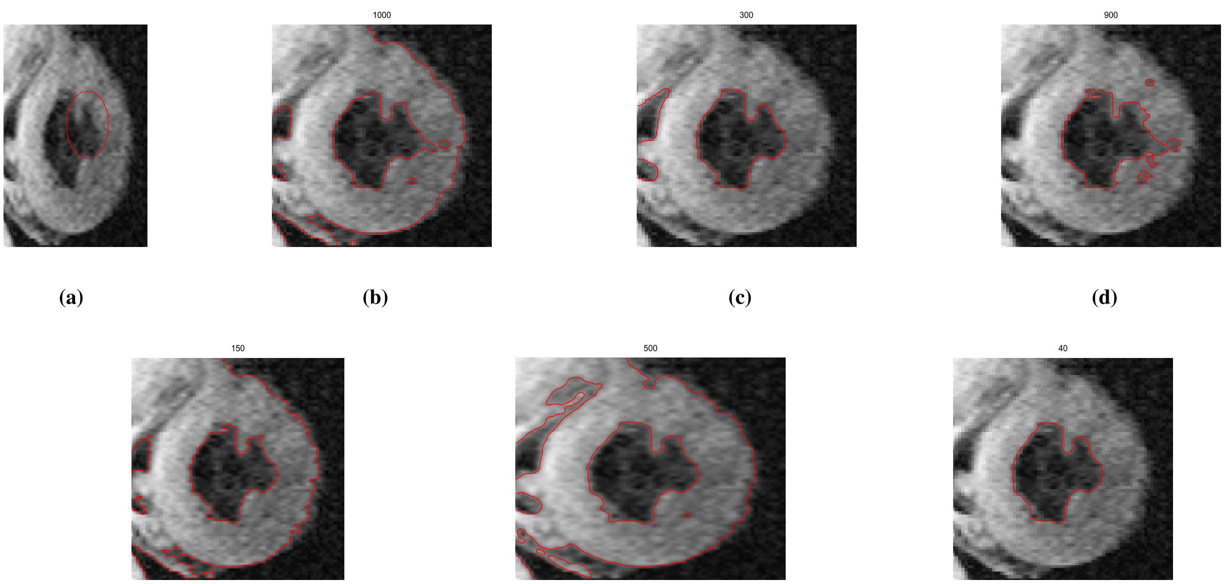

(a) (b) (c) (d)

(e) (f) (g)

FIGURE 6. Segmentation of left ventricle of heart in CMR image with intensity inhomogeneity, noise and complex background (a) original image with initial contour and (b)-(g) shows the segmented results by SBGFRLS, LGDF, CVES, HRSPF, GLSPF and proposed models.

So these parameters should be selected properly. For this particular experiment, parameters used for SBGFRLS model are $\sigma = 13$ and $\alpha = 25$, for LGDF model parameters used are $\sigma = 5$ and $\alpha = 20$, for CVES model parameter used is $\alpha = 0.01$, for HRSPF model parameter used is $\sigma = 16$ and for proposed model parameters used are $\sigma = 15$ and $\alpha = 20$.

We have also tested the proposed model on different real dataset of MRI slices of different patients having tumor of different size taken from web (MNI BITE) as well as from hospital in Peshawar, Pakistan. In Fig. 9 the images in first and second columns are in the axial plane of different patient taken from MNI BITE dataset [20] whereas the images in third and forth columns are in sagittal and axial plane respectively and are of same patient taken from local hospital in Peshawar, Pakistan. The final segmented results of MRI images are given in Fig. 9 showed that the proposed model has successfully segmented tumor in all MRI images. The

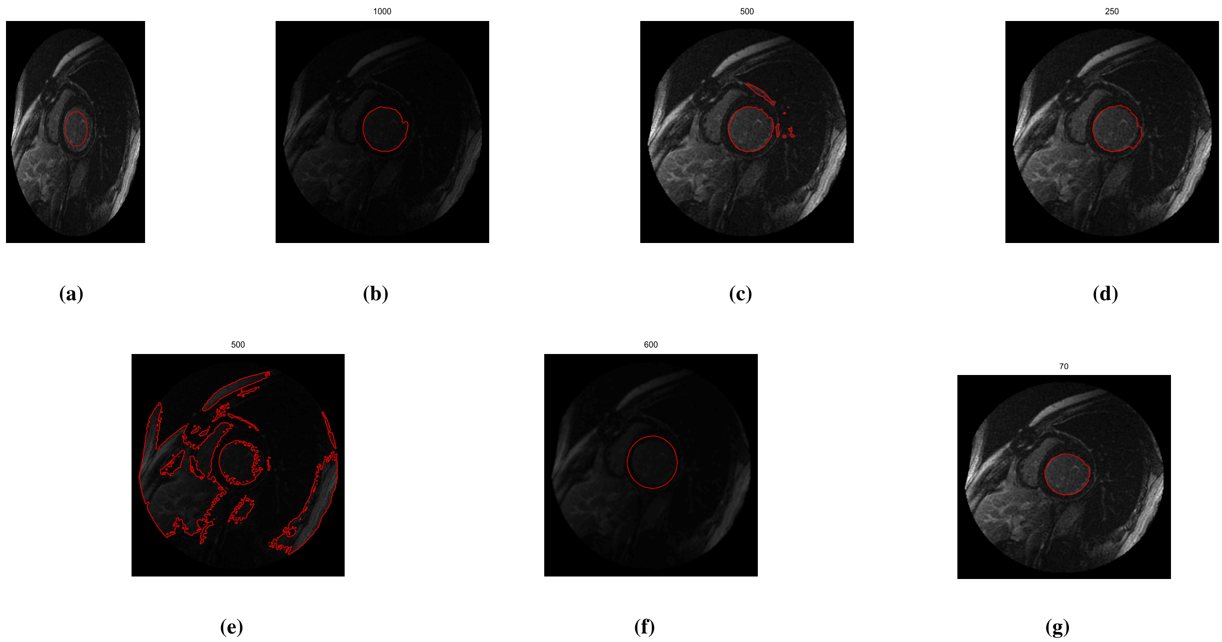

(a) (b) (c) (d)

(e) (f) (g)

FIGURE 7. Comparison of proposed model for segmenting a Cardiac magnetic resonance image taken from dataset Radau *et al.* [21] which has intensity inhomogeneity and background having minimum intensity (a) original image with initial contour and (b)-(g) shows the segmented results by SBGFRLS, LGDF, CVES, HRSPF, GLSPF and proposed models.

TABLE 3. Comparisons of Jaccard Similarity of SBGFRLS, LGDF, CVES, HRSPF and GLSPF models with the proposed model.

Models	Fig. 1	Fig. 2	Fig. 3	Fig. 4	Fig. 5	Fig. 6	Fig. 7
$SBGFRLS$	0.5521	0.2899	0.5357	0.5866	0.5834	0.896	0.880
$LGDF$	0.324	0.6913	0.8547	0.5222	0.7891	0.787	0.899
$CVES$	0.731	0.756	0.823	0.622	0.612	0.832	0.783
$HRSPF$	0.0228	0.5809	0.5357	0.4866	0.5542	0.2861	0.5995
$GLSPF$	0.0442	0.4809	0.4673	0.4300	0.4746	0.6660	0.3245
$Proposed$	0.995	0.993	0.997	0.999	0.995	0.999	0.994

tumor is accurately segmented in all MRI image showing its capability of dealing with inhomogeneous medical images.

B. QUANTITATIVE RESULTS

This section discuss the quantitative results of the proposed model in terms of number of iterations vs CPU time and Jaccard Similarity index (JSI). Firstly, we have given a comparison of the proposed model with SBGFRLS, LGDF, CVES, HRSPF and GLSPF models in terms of number of iterations and CPU time in seconds (Table 1). is revealed from the comparison that proposed model is fast in convergence as compared to SBGFRLS, LGDF, CVES, HRSPF and GLSPF models. All the experiments are done with best values of parameters, which are considered by hit and trial method. Furthermore, the proposed model is compared with SBGFRLS, LGDF, CVES, HRSPF and GLSPF models with images having intensity inhomogeneity and complex background of large sizes. In Table 2, number of iterations and CPU time in seconds is given for images of different sizes. It can be observed from the table that the proposed model has segmented images of large sizes in less iterations and CPU time as compare to the other models discussed.

Next, quantitatively better performance of the proposed model in comparison with SBGFRLS, LGDF, CVES, HRSPF and GLSPF models is discuss. The segmentation efficiency of each model is checked by Jaccard similarity index (JSI), which is given by: $JSI(A_1, A_2) = \frac{(|A_1 \cap A_2|)}{(|A_1 \cup A_2|)}$, where A_1 is the final segmented image and A_2 is the ground truth which is obtained by manual segmentation. A model whose JSI value is close to 1 may be considered as a better segmentation model. Table 3 shows the JSI values of all four models for images given in Fig. 2 to 8, where the proposed model has given better JSI value as compared to other three models. For finding JSI value in all experiments the optimal value of parameters has used. Thus it is concluded that proposed model has produced better segmentation results in images having inhomogeneous intensity with complex background, which usually occur in medical images.

Remark 1: The proposed model is tested on a set of images from two different types of databases, where the JSI has a confidence interval 0.9 ± 0.07.

Table 4 shows the quantitative analysis of the experimental results in terms of evaluation metrics. The evaluation metrics are used to evaluate the performance of SBGFRLS, LGDF, CVES, HRSPF, GLSPF and proposed models by comparing tumors with the ground truths created by human experts, including Sensitivity (SE), Specificity (SP), Accuracy (AC), Dice Similarity Coefficient (DSC). These metrics are defined as:

$$SE = W_{TP}/(W_{TP} + W_{FN}),$$

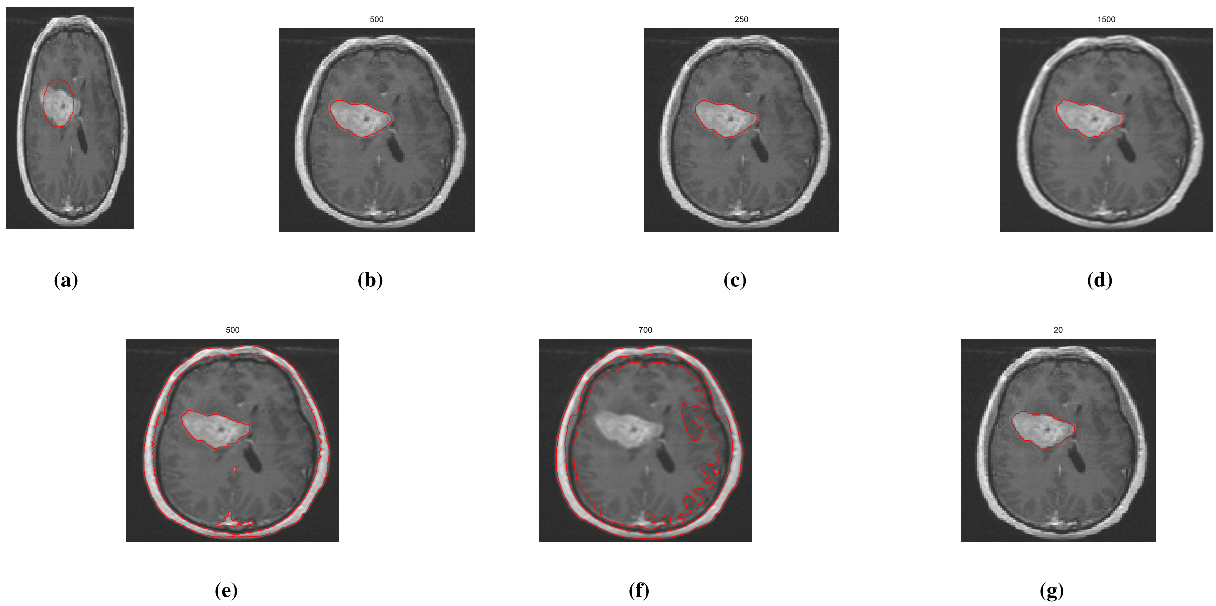

FIGURE 8. Comparison of our model with other existing models on MRI image, where all the model produced better results, the proposed model has produced better results is terms of number of iterations and CPU time (a) original image with initial contour and (b)-(g) shows the segmented results by SBGFRLS, LGDF, CVES, HRSPF, GLSPF and proposed models.

$$\begin{aligned} SP &= W_{TN}/(W_{TN} + W_{FP}), \\ AC &= (W_{TP} + W_{TN})/(W_{TP} + W_{TN} + W_{FP} + W_{FN}), \\ DSC &= 2W_{TP}/(2W_{TP} + W_{FN} + W_{FP}). \end{aligned}$$

where W_{TP}, W_{TN}, W_{FP} and W_{FN} indicate the number of true positives, true negatives, false positives and false negatives respectively.

V. APPLICATION OF PROPOSED MODEL ON DIFFERENT MEDICAL IMAGES

A. TEST ON MRI AND MAMMOGRAM IMAGES

The proposed model is tested on MRI and Mammogram images taken from real data set collected and Website with severe inhomogeneous intensity. Our proposed model efficiently and successfully extract the region of interest (tumor) and give clear segmented results as shown in Fig. (10a- 10d).

Figure 11 shows the final segmentation results on set of brain MRI images taken from the data set of the local hospital in Pakistan. The first column shows the original image with initial contour and the second column shows the final segmented results. These images are corrupted with severe intensity inhomogeneity and have low contrast and weak edges. Due to these factors the segmentation of these medical images with tumor are very hard to segment. But clearly it can be seen that our proposed model is able to accurately detect and segment the edges of region of interest i.e. tumors and also outperformed very well in all images as shown in Fig. 11.

In Fig. 12 the brain MRI image of Fig. 4 can be used for five different positions of initial contours that can be set inside and across the edges of a region of interest. First row in Fig. 12, shows the original image with different initial contours. Row 12b shows the segmentation results of SBGFRLS model, row 12c shows the segmentation results of LGDF model, row 12d shows the segmentation results of CVES model, row 12e shows the segmentation results of HRSPF model, row 12f shows the segmentation results of GLSPF model and last row 12g shows the final segmentation results of proposed model. From the segmentation results it demonstrate that our proposed model efficiently segment the region of interest having intensity inhomogeneity for different positions of initial contours, whereas the existing models are even not able to segment the region of interest as well as sensitive to the initial contour.

B. TEST ON ULTRASOUND AND CMR IMAGES

Further, images of ultrasound acquired from the Website and CMR from dataset Radau *et al.* [21] are also considered to assess the performance of the proposed model. The proposed model is able to segment the region of interest properly and showing its capability of dealing with inhomogeneous medical images as shown in Fig. 13.

C. APPLICATION OF PROPOSED MODEL ON NOISY IMAGES

Figure 14 illustrates the final segmentation results of real noisy images by proposed model. Fig. 14a shows the original image having tumor and Fig. 14b, 14c, 14d, 14e, 14f, 14g, 14h shows the image which are corrupted by zero mean Gaussian noise with different standard deviation values i.e. 0.05, 0.08, 0.005, 0.008, 0.1, 0.4 and 0.6 respectively. The final segmentation results shows that the proposed model efficiently detect tumor in all images in the presence of Gaussian noise. Even

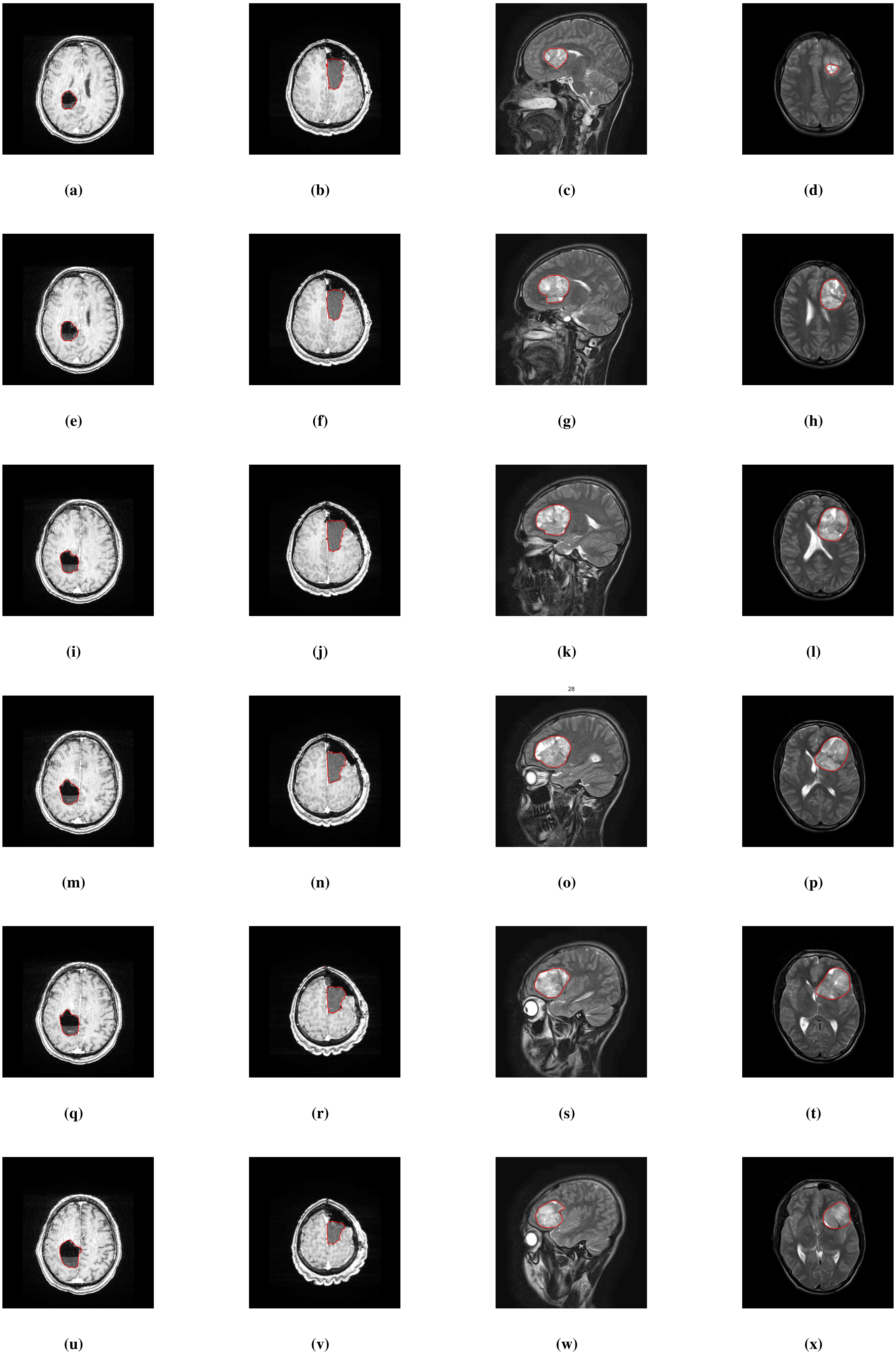

FIGURE 9. Segmentation results of the proposed model in brain MRI data set of a different patients. The images in first and second columns are in the axial plane, while the images in third column are in sagittal plane and forth column are in axial plane.

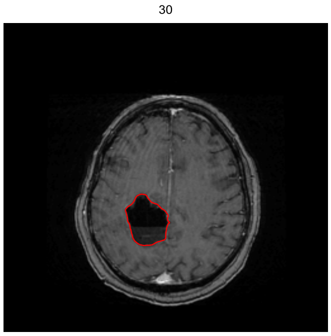

(a) Brain MRI Image

(b) Mammogram Image

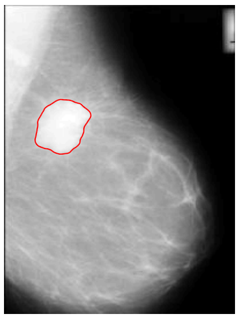

(c) Mammogram Image

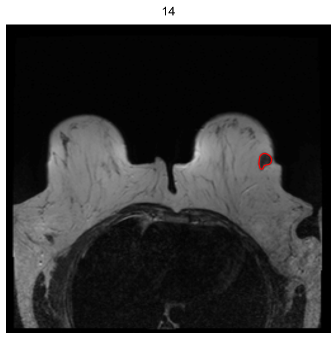

(d) Mammogram Image

FIGURE 10. **Final segmentation result of the proposed model on (a) brain MRI image taken from [20] (b-d) Mammogram images taken from Website and local hospital of Pakistan.**

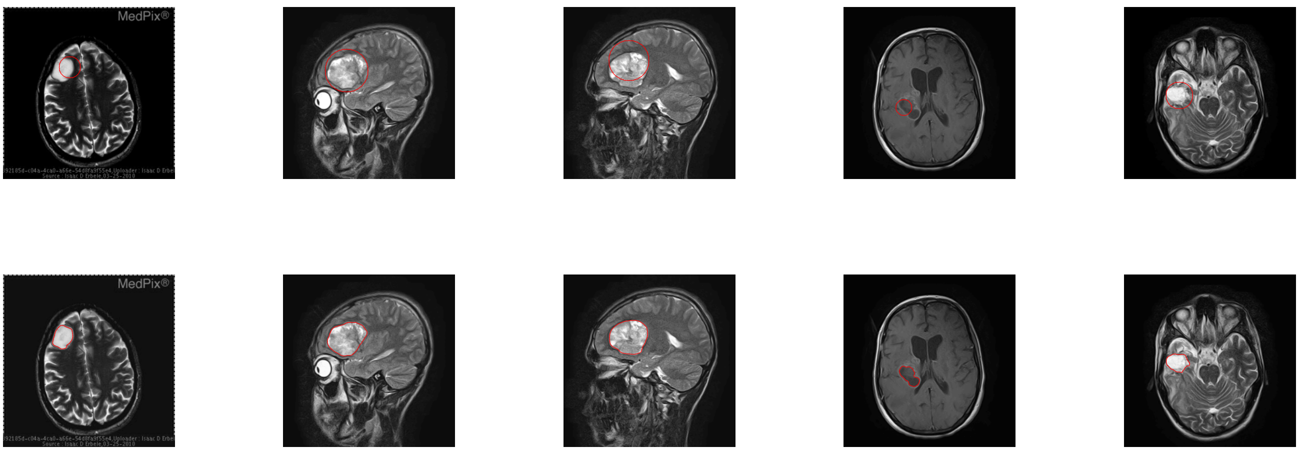

FIGURE 11. **Segmented results of our proposed model for medical images having inhomogeneous intensity: First row: original images with different initial contours. Second row: Final segmented results.**

in presence of severe noise the proposed model is also able and performed well to segment the desired tumor.

Figure 8 shows the brain MRI image of Fig. 15 that can be used with salt and pepper noise and weak boundaries. Fig. 15a, 15b, 15c, 15d, 15e shows the salt and pepper noise with different noise densities, i.e. 0.05, 0.08, 0.09, 0.1, 0.2 and 0.3 respectively. The proposed model is capable of handling and accurately segment tumor having salt and pepper noise with different noise densities and yields adequate results of segmentation for both Gaussian noise as well as for salt and pepper noise.

D. PARAMETER SENSITIVITY

In this section, we give a brief discussion about the sensitivity of the proposed model on a parameter σ. σ is one of the important parameters, which can affect the segmentation results of medical images. In order to test the dependence of

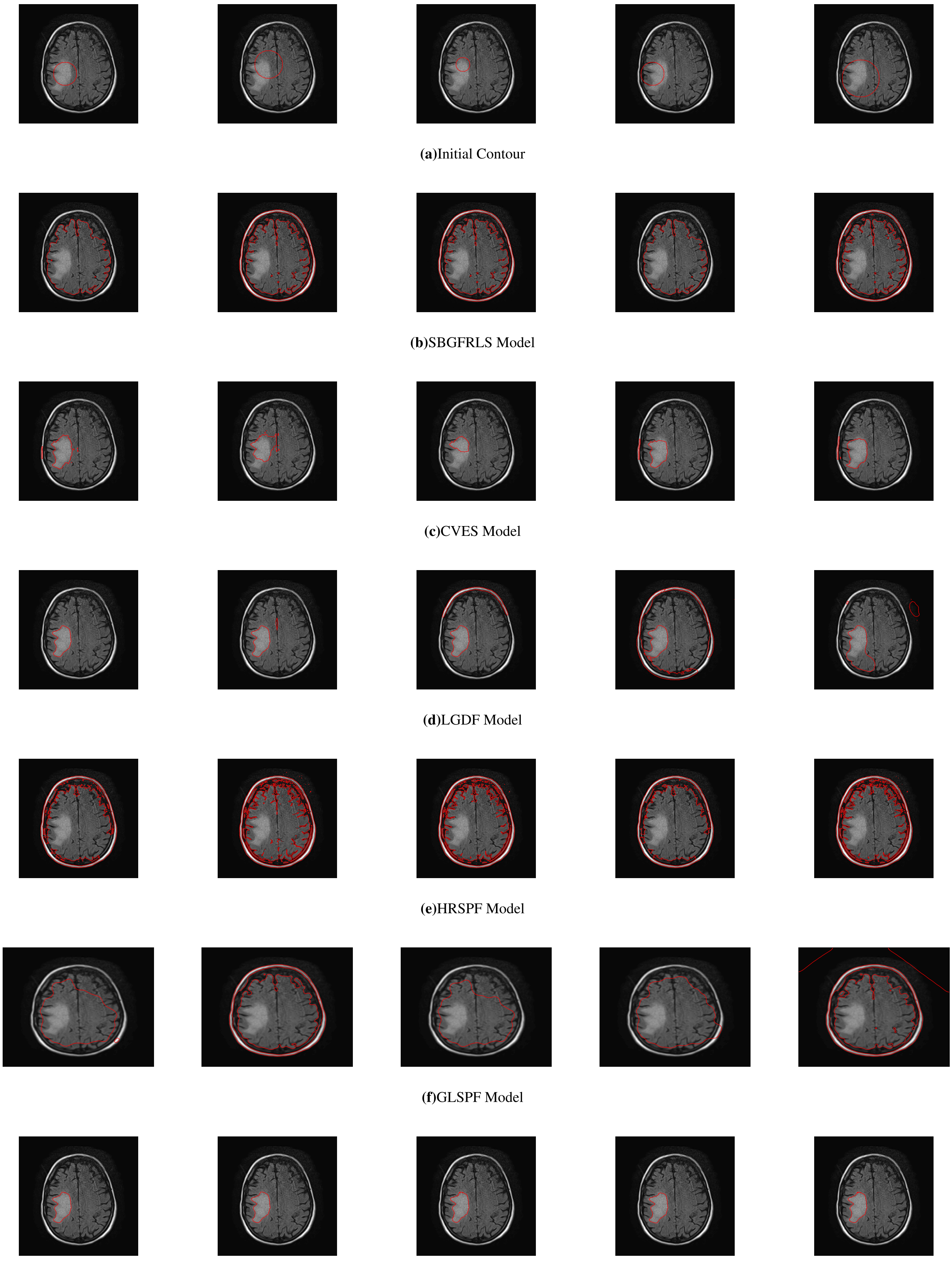

FIGURE 12. Segmentation results on MRI real image by proposed method: (a): Original image with different initial contours. (b)-(g): Final segmentation results of SBGFRLS, LGDF, CVES, HRSPF, GLSPF and proposed models.

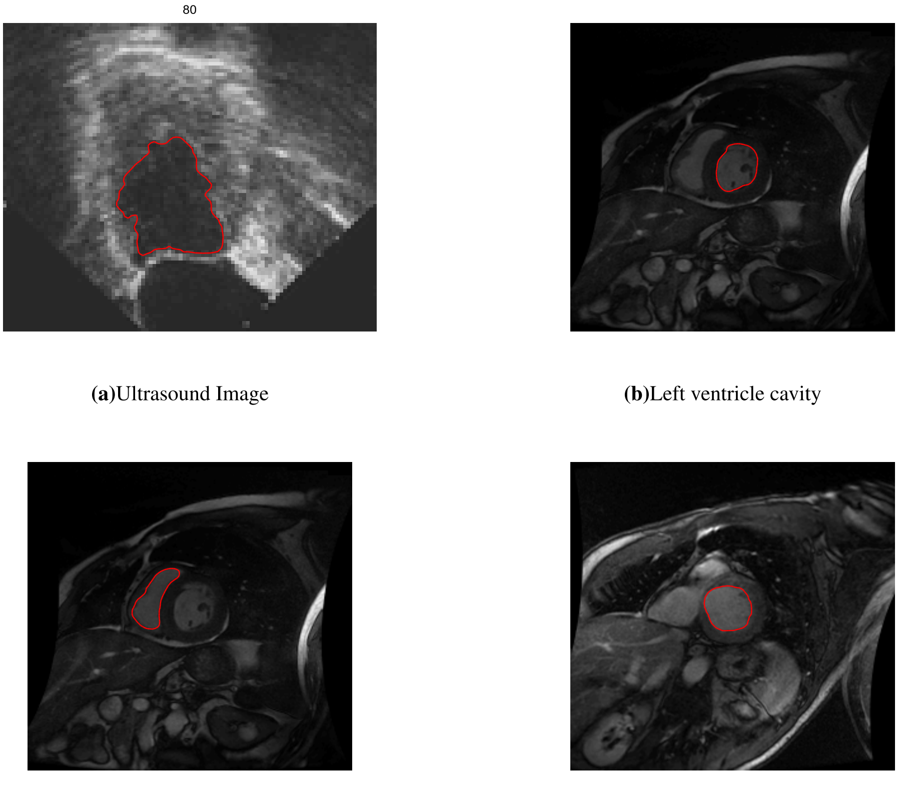

(a) Ultrasound Image **(b)**Left ventricle cavity

(c) Right ventricle cavity **(d)**Left ventricle cavity

FIGURE 13. Final segmentation results on Ultrasound image of left ventricle taken from Website and a set of Cardiac magnetic resonance images taken from dataset Radau *et al.* [21].

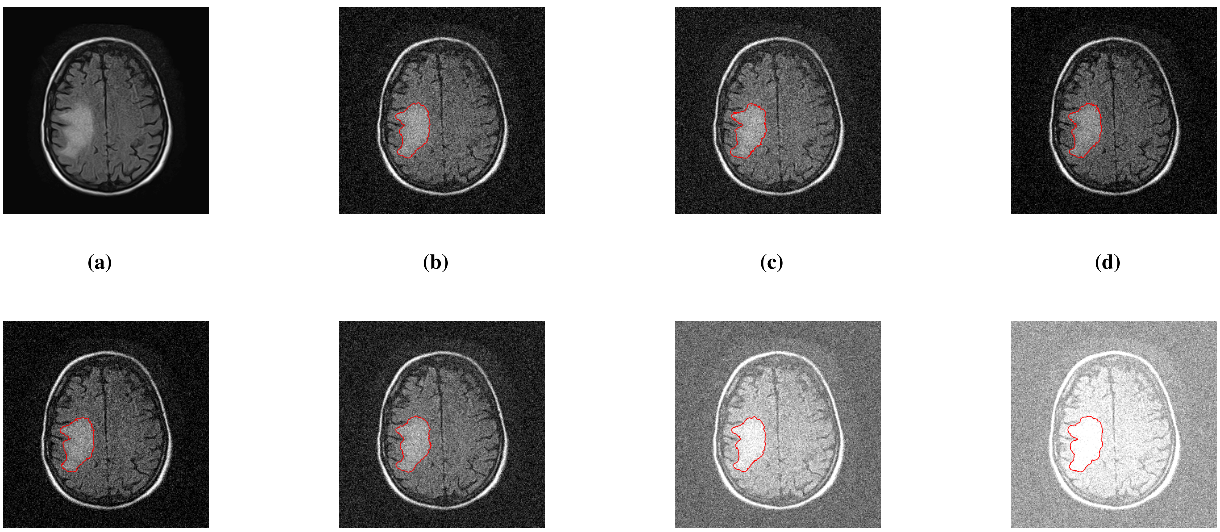

(a) (b) (c) (d)

(e) (f) (g) (h)

FIGURE 14. Final segmentation results of real noisy medical image by the proposed model (a) Original image and (b-h) Given image with different standard deviation 0.05, 0.08, 0.005, 0.008, 0.1, 0.4 and 0.6 respectively.

the proposed model on σ, various experiments are carried out. Here we show three experiments on different images given in Fig. 4, 5 and 8 in which JSI is plotted against different values of σ. Where it can be seen from Fig 16a and 16b for images in Fig. 4 and 5 the best value of σ are 12 and 5 to get the best Jaccard value. Best value of σ for image in Fig. 8

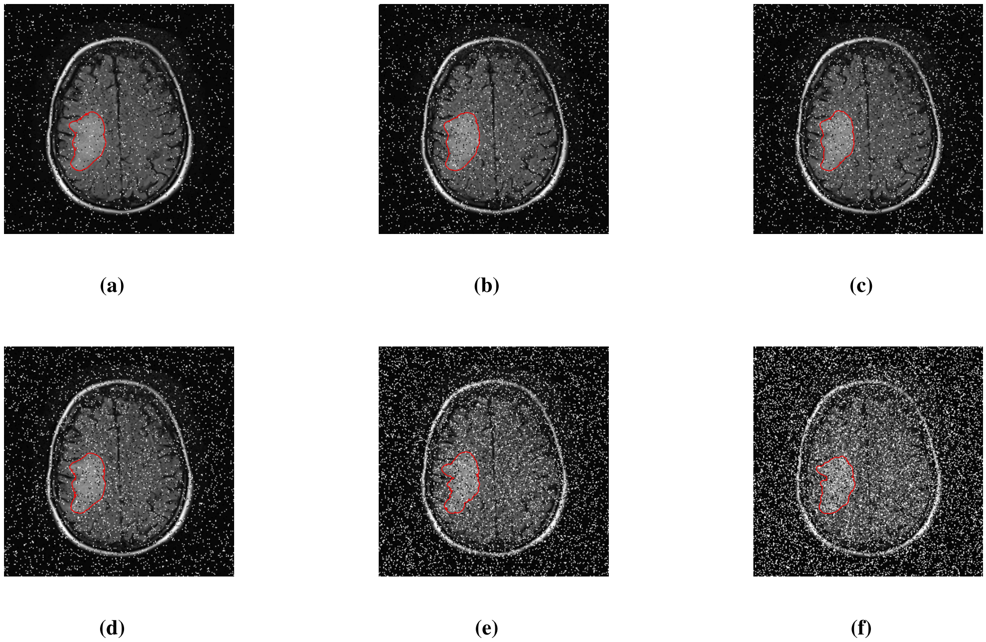

FIGURE 15. **Final segmentation results of real medical image with salt and pepper noise.**

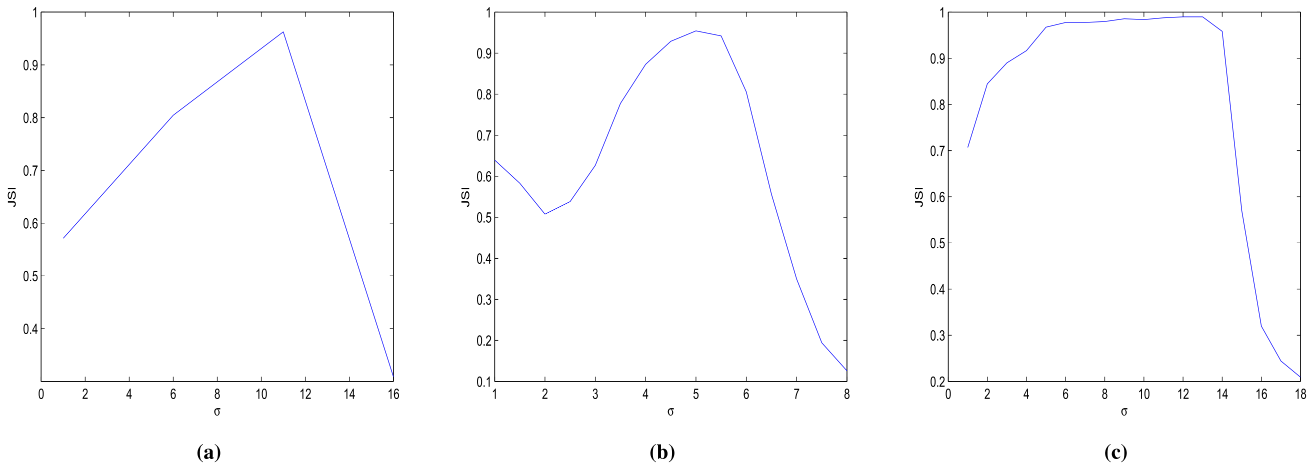

FIGURE 16. **Sensitivity of proposed model on a parameter σ for images given in Fig. 4, 5 and 8.**

is between 11.7 and 13.8, where optimal Jaccard value is obtained as shown in Fig. 16c.

VI. CONCLUSION

In this paper, a novel active contour model is proposed to segment structure of tumor in medical images intensity inhomogeneity. The proposed model with new statistic is developed by introducing coefficient of variation in probability density function. By using relative statistic, squared coefficient of variation in the data fitting term to attain local intensity information of the image which gives better segmentation results in medical images having inhomogeneous intensity. The proposed model has produced good results in challenging images having tumor with severe inhomogeneous intensities and also having complex background. The proposed model is tested on different type of other medical images to show that the object of interest is approximately similar to the ground truth and also the results are compared with the existing state of the art models in terms of both qualitatively and quantitatively. The quantitative results of the proposed model indicate that the segmented region of interest is approximately similar to the ground truth and prove the best values of JSI, sensitivity, specificity, accuracy and dice similarity coefficient. The proposed model is tested on different medical images taken from different databases. The proposed model is also able to handle the images having severe noise.

A. LIMITATIONS

The proposed model has certain limitations. Firstly, the proposed model should be improved for large size medical

TABLE 4. The calculated segmentation evaluation metrics of SBGFRLS, LGDF, CVES, HRSPF, GLSPF and proposed models in terms of SE, SP, AC and DSC.

Images	Models	W_{TP}	W_{FP}	W_{TN}	W_{FN}	SE	SP	AC	DSC
Fig. 1	SBGFRLS	2286	523	254249	242	0.9043	0.9979	0.9970	0.8567
	LGDF	2388	7258	247514	140	0.9446	0.9715	0.9712	0.3923
	CVES	2000	850	254200	250	0.9123	0.9961	0.9866	0.8840
	HRSPF	0	112050	1084	144166	0.0289	0.0351	0.0777	0.0445
	GLSPF	0	112060	1044	144196	0.0204	0.0823	0.0754	0.0324
	Proposed	2481	24	254659	136	0.9586	0.9999	0.9994	0.9688
Fig. 2	SBGFRLS	757	488	15410	1297	0.3693	0.9693	0.9006	0.4589
	LGDF	1929	591	15307	125	0.9391	0.9628	0.9601	0.8435
	CVES	1905	530	15100	417	0.7324	0.9453	0.9500	0.8898
	HRSPF	19	764	15390	1779	0.5849	0.6721	0.8972	0.8103
	GLSPF	2	1390	13817	2743	0.5234	0.6200	0.8219	0.7011
	Proposed	1999	66	15778	109	0.9508	0.9958	0.9965	0.9423
Fig. 3	SBGFRLS	1314	627	63083	512	0.7196	0.9902	0.9826	0.6976
	LGDF	1753	225	63485	73	0.9600	0.9965	0.9955	0.8547
	CVES	1210	720	62756	820	0.6543	0.9375	0.9632	0.7848
	HRSPF	5	1161	63291	1076	0.7236	0.9102	0.8841	0.5321
	GLSPF	0	851	63223	1462	0.7010	0.9236	0.8265	0.5023
	Proposed	1810	16	63675	35	0.9988	0.9931	0.9972	0.9920
Fig. 4	SBGFRLS	474	223	64728	111	0.8103	0.9966	0.9949	0.7395
	LGDF	576	518	64433	9	0.9846	0.9920	0.99920	0.6861
	CVES	453	365	64518	200	0.7425	0.8543	0.8047	0.7952
	HRSPF	243	18110	19760	27423	0.0345	0.0736	0.0143	0.0498
	GLSPF	220	19534	16790	28992	0.0298	0.0653	0.0296	0.0329
	Proposed	580	5	64945	6	0.9992	0.9987	0.9995	0.9990
Fig. 5	SBGFRLS	1240	150	63227	919	0.5834	0.9968	0.9864	0.7369
	LGDF	2132	21782	41550	72	0.9601	0.6561	0.6665	0.1633
	CVES	1252	550	63034	700	0.9123	0.5495	0.7415	0.3433
	HRSPF	560	1381	62329	1266	0.3067	0.9783	0.9596	0.2973
	GLSPF	454	1487	62223	1372	0.2486	0.9767	0.9564	0.2410
	Proposed	2146	14	63324	52	0.9673	0.9997	0.9984	0.9756
Fig. 6	SBGFRLS	333	184	12298	156	0.6810	0.9853	0.9738	0.6620
	LGDF	479	10	12472	10	0.9796	0.9877	0.9992	0.9897
	CVES	401	70	12420	80	0.9630	0.9787	0.9988	0.9747
	HRSPF	245	2740	6327	3659	0.5649	0.854	0.9123	0.6219
	GLSPF	384	1899	9990	698	0.7654	0.8349	0.9005	0.8621
	Proposed	485	4	12479	3	0.9987	0.9997	0.9997	0.9959
Fig. 7	SBGFRLS	687	35	64325	489	0.5849	0.9989	0.9924	0.7349
	LGDF	1100	35482	28876	78	0.9338	0.4487	0.4574	0.0583
	CVES	666	95	64310	465	0.6210	0.9980	0.9814	0.7531
	HRSPF	278	967	62743	1548	0.1522	0.9848	0.1810	0.2995
	GLSPF	0	121	63589	1826	0	0.0231	0.0164	0.0032
	Proposed	1180	8	64333	15	0.9728	0.9999	0.9984	0.9656

images (for example 2048 x 2048) having severe inhomogeneity and noise. Secondly, the proposed model should be improved to extract the object of interest and avoid local minima in medical images having texture.

REFERENCES

[1] L. Wang, L. He, A. Mishra, and C. Li, "Active contours driven by local Gaussian distribution fitting energy," *Signal Process.*, vol. 89, no. 12, pp. 2435–2447, Dec. 2009.

[2] W. Cui, Y. Wang, T. Lei, Y. Fan, and Y. Feng, "Level set segmentation of medical images based on local region statistics and maximum *a posteriori* probability," *Comput. Math. Methods Med.*, vol. 2013, pp. 1–12, 2013.

[3] A. Azizi and K. Elkourd, "Fast region-based active contour model driven by local signed pressure force," *Electron. Lett. Comput. Vis. Image Anal.*, vol. 15, no. 1, pp. 1–13, 2016.

[4] V. Caselles, R. Kimmel, and G. Sapiro, "Geodesic active contours," *Int. J. Comput. Vis.*, vol. 22, no. 1, pp. 61–79, 1997.

[5] T. F. Chan and L. A. Vese, "Active contours without edges," *IEEE Trans. Image Process.*, vol. 10, no. 2, pp. 266–277, 2001.

[6] X. F. Wang, D. S. Huang, and H. Xu, "An efficient local Chan–Vese model for image segmentation," *Pattern Recognit.*, vol. 43, no. 3, pp. 603–618, 2010.

[7] S. Liu and Y. Peng, "A local region-based Chan–Vese model for image segmentation," *Pattern Recognit.*, vol. 45, no. 7, pp. 2769–2779, Jul. 2012.

[8] C. Li, C.-Y. Kao, J. C. Gore, and Z. Ding, "Implicit active contours driven by local binary fitting energy," in *Proc. IEEE Conf. Comput. Vis. Pattern Recognit.*, Jun. 2007, pp. 1–7.
[9] B. Wu and Y. Yang, "Local- and global-statistics-based active contour model for image segmentation," *Math. Problems Eng.*, vol. 2012, pp. 1–16, Jan. 2012.
[10] C. Li, C.-Y. Kao, J. C. Gore, and Z. Ding, "Minimization of region-scalable fitting energy for image segmentation," *IEEE Trans. Image Process.*, vol. 17, no. 10, pp. 1940–1949, Oct. 2008.
[11] L. Wang, H. Zhang, K. He, Y. Chang, and X. Yang, "Active contours driven by multi-feature Gaussian distribution fitting energy with application to vessel segmentation," *PLoS ONE*, vol. 10, no. 11, pp. 1–18, 2015.
[12] D. B. Mumford and J. Shah, "Optimal approximations by piecewise smooth functions and associated variational problems," *Commun. Pure Appl. Math.*, vol. 42, no. 5, pp. 577–685, 1989.
[13] N. Badshah, K. Chen, H. Ali, and G. Murtaza, "Coefficient of variation based image selective segmentation model using active contours," *East Asian J. Appl. Math.*, vol. 2, no. 2, pp. 150–169, May 2012.
[14] K. Zhang, L. Zhang, H. Song, and W. Zhou, "Active contours with selective local or global segmentation: A new formulation and level set method," *Image Vis. Comput.*, vol. 28, no. 4, pp. 668–676, Apr. 2010.
[15] Y. Boutiche and M. Halimi, "The performance of some implicit region-based active contours in segmenting and restoring welding radiographic images," *Russian J. Nondestruct. Test.*, vol. 53, no. 10, pp. 731–743, Oct. 2017.
[16] S. Gao and T. D. Bui, "Image segmentation and selective smoothing by using mumford-shah model," *IEEE Trans. Image Process.*, vol. 14, no. 10, pp. 1537–1549, Oct. 2005.
[17] S. Soomro, A. Munir, and K. N. Choi, "Hybrid two-stage active contour method with region and edge information for intensity inhomogeneous image segmentation," *PLoS ONE*, vol. 13, no. 1, Jan. 2018, Art. no. e0191827, doi: 10.1371/journal.pone.0191827.
[18] J. Fang, H. Liu, L. Zhang, J. Liu, and H. Liu, "Active contour driven by weighted hybrid signed pressure force for image segmentation," *IEEE Access*, vol. 7, pp. 97492–97504, 2019.
[19] H. Liu, J. Fang, Z. Zhang, and Y. Lin, "A novel active contour model guided by global and local signed energy-based pressure force," *IEEE Access*, vol. 8, pp. 59412–59426, 2020.
[20] *The MNI BITE Database*. [Online]. Available: http:www.bic.mni.mcgill.ca/~laurence/data/
[21] P. Radau, Y. Lu, K. Connelly, G. Paul, A. J. Dick, and G. A. Wright, "Evaluation framework for algorithms segmenting short axis cardiac MRI," *MIDAS J.-Cardiac MR Left Ventricle Segmentation Challenge*. Accessed: 2019. [Online]. Available: http://hdl.handle.net/10380/3070

NOOR BADSHAH received the Ph.D. degree in mathematics from the University of Liverpool, U.K. He is currently an Associate Professor with the Department of Basic Science, University of Engineering and Technology Peshawar, Pakistan. His current research interests include modeling in image processing, biology, and computational mathematics.

HADIA ATTA received the master's degree in mathematics from Shaheed Benazir Bhutto Women University, Peshawar, Pakistan, in 2008, and the M.S. degree in mathematics from the University of Engineering and Technology, Peshawar, in 2014. She is currently pursuing the Ph.D. degree with the Department of Mathematics, Islamia College Peshawar, Pakistan. She is also an Assistant Professor with the Islamia College Peshawar. Her current research interests include image processing, image segmentation, and computational mathematics.

SYED INAYAT ALI SHAH received the M.Sc. and M.Phil. degrees in mathematics from Quaid-e-Azam University, Islamabad, Pakistan, in 1987 and 1990, respectively, and the Ph.D. degree in mathematics from Saga University, Japan, in 2002. Since 2010, he has been with the Department of Mathematics, Islamia College Peshawar, Pakistan, where he is currently a Professor. His research interest includes algebraic number theory.

SOBIA ATTAULLAH received the master's degree in zoology from the Department of Zoology, University of Peshawar, Pakistan, in 2001, the M.Phil. degree from the Kohat University of Science and Technology, Kohat, Pakistan, in 2010, and the Ph.D. degree from the Islamia College Peshawar, Pakistan, in 2017. She is currently with the Islamia College Peshawar as an Assistant Professor. Her current research interests include molecular biology and image segmentation.

NASRU MINALLAH (Member, IEEE) received the B.Sc. degree in computer engineering from the University of Engineering and Technology Peshawar, Pakistan, in 2004, the M.Sc. degree in computer engineering from the Lahore University of Management Sciences, Lahore, Pakistan, in 2006, and the Ph.D. degree from the Communications Group, School of Electronics and Computer Science, University of Southampton, Southampton, U.K., in 2010. He is currently an Associate Professor with the Department of Computer Systems Engineering, University of Engineering and Technology Peshawar. His research interests include image processing, remote sensing, low-bit-rate video coding for wireless communications, turbo coding and detection, and iterative source-channel decoding.

MATI ULLAH is currently pursuing the Ph.D. degree with the Department of Basic Sciences, University of Engineering and Technology Peshawar, Pakistan. His research interests include joint image restoration and segmentation model of color images.